

Modeling of hydration of cement-based composed binders: phenomenological approach

L. Buffo-Lacarrière^{1,2}, A. Sellier², G. Escadeillas², A. Turatsinze²

¹ VINCI Construction Grands Projets, Rueil-Malmaison, France;

² Laboratoire Matériaux et Durabilité des Constructions, Toulouse, France

1. Introduction

As the use of composed binders instead of pure clinker is increasingly being recommended for durable construction, accurate knowledge of the hydration development of these new binders is necessary to correctly predict early age behavior of structures. Models described in the literature use separate laws for clinker and for the reactions of additions. For instance, De Schutter [1] propose s a model of hydration for cements composed of clinker and slag and Kishi [2] model s hydration for cement mixed with fly ash. These models reproduce the combined hydrations of these species well, but do not explicitly take account of the effect of water content on hydration. This effect is nevertheless very important since it modifies not only the final degree of hydration [3, 4], but also the hydration kinetics. It cannot be neglected for a realistic prevision of concrete hydration in structures. These considerations led us to develop an original composed-binder hydration model able to take account of coupling with the effects of water content variations.

2. Chemo-physical observations

The hydration kinetics is the result of two antagonistic physical phenomena. On the one hand supersaturation of the interstitial solution accelerates hydrate precipitation [5] and thus increases the global hydration kinetics. On the other hand, as hydration reactions are possible only if water and reactive ions are present, the hydration kinetics is decreased by the difficulty of contact between water and anhydrous grains surrounded by a hydrated layer.

In the first stages of hydration, as only a few solid hydrated phases have been produced, the hydration kinetics is mainly driven by supersaturation. Then, beyond a critical degree of hydration, a decrease of the kinetics due to hydrate formation will become preponderant as , with the increasing degree of hydration, the hydrate layers surrounding the anhydrous grains progressively separate the reacting anhydrous phase from the water.

Some authors [3, 4] note another consequence of hydrate formation. The hydration kinetics is also reduced by the closing of pores and hydration reactions can even be stopped if there is not enough space available for hydrate development (closed porosity).

The case of water content effects on hydration development is more complex. In the first stages of hydration, low water content accelerates supersaturation of the interstitial solution and consequently the hydration kinetics. Then (at ages of 1 day and beyond [6]), low water content reduces the hydration kinetics and can even stop reactions.

3. Equations

In addition to these chemo-physical effects, reactions of dissolution and hydrate formation are modified by environmental conditions (temperature and relative humidity of the surrounding air for instance). This leads us to propose a multiphasic model able to reproduce all these interactions between environment and hydration. The evolution of hydration degrees (Eq. 1) is thus coupled with the water mass balance equation (Eq. 2) and heat balance equation (Eq. 3).

$$\frac{\partial \alpha_i}{\partial t} = F(\alpha_i, W, T) \quad (1)$$

$$\frac{\partial W}{\partial t} = \text{div}(-D_w \cdot \overrightarrow{\text{grad}} W) + Q_{th}^W \cdot \alpha_i \quad (2)$$

$$r \cdot c \cdot \frac{\partial T}{\partial t} = \text{div}(-l \cdot \overrightarrow{\text{grad}} T) + Q_{th}^T \cdot \alpha_i \quad (3)$$

Where: - $X = (X_1 \cdot X_2 \cdot X_n)$ and (i=1 → clinker, i=2..n → pozzolanes)

- α_i is the degree of hydration of phase "i"
- W is the total water content of concrete
- D_w is the water transfer coefficient
- $Q_{th_i}^W$ is the water needed for total hydration of phase "i"
- T is temperature
- l is thermal conductivity
- r and c are concrete density and specific heat
- $Q_{th_i}^T$ is the heat produced by complete hydration of phase "i"

The hydration law modeled by the function F represents the reaction kinetics of each of the binder components (clinker, fly ash, silica fume ...). According to the chemo-physical considerations presented in the previous paragraph the following equation (Eq. 4) is proposed.

$$\frac{\partial \alpha_i}{\partial t} = A_i \cdot c_i(\alpha_i, W) \cdot \Pi_i(r_{mi}) \cdot h_i(T) \cdot g_i \quad (4)$$

Where A_i is a fitting parameter linked to the acceleration of the reaction kinetics due to supersaturation.

3.1. Chemical activation

Thus, we propose first a function modeling the particular effect of water in the first stage of reactions: function c_i represents the chemical activation due to supersaturation of the interstitial solution.

It is assumed that the activation of kinetics increases linearly with the hydration degree, which leads to the following expression for c_i (Eq. 5). In other words, we suppose that the ratio between dissolution speed and reactive consumption speed is in favor of supersaturation.

$$c_i = \frac{V_{An\,diss_i}}{V_W} = \frac{a_i \cdot V_{An\,0_i}}{V_W} \quad (5)$$

Where: - $V_{An\,diss_i}$ is the volume of dissolved anhydrous phase "i"

- $V_{An\,0_i}$ is the initial volume of anhydrous phase "i"

- V_W is the volume of water

3.2. Water accessibility to anhydrous phase

The function Π_i in Eq. (4) expresses the decrease in hydration kinetics occurring due to a sufficient degree of hydration.

The chemo-physical observations developed in paragraph 2 highlight the fact that it is the accessibility of water to the anhydrous phase that governs the hydration kinetics decrease. The notion of accessibility combines the influences of water content, porosity, and thickness of hydrate layers.

We chose to model the decrease in hydration kinetics caused by difficulty of contact between the anhydrous phases and water by a single parameter Π defined as a function of the mean normalized distance between these two phases (\bar{r}_m).

This function will become preponderant against increasing function c for sufficient degrees of hydration.

$$\Pi_i = \exp\left(-B_i \cdot \bar{r}_{m_i}^{n_i}\right) \quad (6)$$

Where: - B_i and n_i are calibration parameters

- \bar{r}_{m_i} is defined in Eq. (7) as a function of water content, porosity and solid phases present in the paste.

Inspired by the physical considerations presented in paragraph 2, we chose the following expression (Eq. 7) for the normalized mean distance separating water and an anhydrous phase.

The numerator represents parameters decreasing the kinetics while the denominator contains parameters increasing it.

$$\bar{V}_{m_i} = \frac{C_{P_{hydr_i}} \cdot (1/\Phi_p)}{C_{P_{anh_i}} \cdot W_p} \quad (7)$$

Where: - $C_{P_{hydr_i}}$ is the volumetric concentration in paste of hydrate produced from anhydrous grains of phase "i"

- Φ_p is the porosity of the paste

- $C_{P_{anh_i}}$ is the anhydrous volumetric concentration in paste

- W_p is the volumetric concentration of water in paste

The volumetric concentration of hydrates and the anhydrous phase are determined using Eqs. (8) and (9).

$$C_{P_{hydr_i}} = R_i \cdot a_i \cdot \frac{V_{An0_i}}{V_{paste_{ini}}} \quad (8) \quad \text{and} \quad C_{P_{anh_i}} = (1-a_i) \cdot \frac{V_{An0_i}}{V_{paste_{ini}}} \quad (9)$$

Where - R_i is the volume ratio between hydrates and anhydrous phases for the species "i"

- $V_{paste_{ini}}$ is the initial paste volume (water + anhydrous phases)

Paste porosity is determined by Eq. (10).

$$\Phi_p = 1 - \sum_i (C_{P_{hydr_i}} + C_{P_{anh_i}}) \quad (10)$$

It is interesting to note that it was necessary to use individual parameters in function c_i (Eqs. 4 and 5) in order to reproduce the response of each anhydrous phase to the effects of this activation of kinetics. In contrast, the function Π_i (Eqs. 4, 6 and 7) models the facility of contact between water and the anhydrous grains and uses some parameters which are common to all anhydrous phases. The decrease in hydration kinetics is due to the limitation of water microtransfer (global parameter) between the porosity (global parameter) and the residual anhydrous phase.

3.3. Thermal activation

Temperature effects on the hydration kinetics are taken into account through the function h_i (Eq. 4). For this purpose, Arrhenius' law (Eq. 11), traditionally used to describe the influence of temperature on many chemical and physical processes [7], is applied.

$$h_i = \exp\left(-\frac{E_{a_i}}{RT}\right) \quad (11)$$

Where: - E_{a_i} is the activation energy of phase "i"

- R is the gas constant (8.314 J/mol.K)

3.4. Delaying effect of pozzolanic additions

In the case of pozzolanic component hydration, the reaction kinetics depends on the kinetics of the primary reaction. Indeed the pozzolanic reaction is a secondary reaction which combines the anhydrous phase with portlandite produced by clinker primary reaction.

This interaction between primary and pozzolanic reaction is modeled by a dependence of the pozzolanic hydration kinetics on the portlandite content in the paste (Eq. 12).

$$g_i = \begin{cases} C_{pCH} & \text{if } i = \text{pozzolanic component} \\ 1 & \text{if } i = \text{clinker} \end{cases} \quad (12)$$

Where C_{pCH} is the volumetric concentration of portlandite in the paste.

This portlandite concentration is reevaluated at any calculation time by adding CH production by clinker hydration and deducting CH consumption by pozzolanic additions.

4. Calibration principle

The hydration kinetics law parameters of each anhydrous phase were determined using a quasi adiabatic test performed with a Langavant calorimeter. For calibration, a least squares method was used to determine the material parameters that allowed the experimental hydration heat curve to be reproduced. Thus, a calibrated law was obtained by using only heat cumulated results of the quasi adiabatic test on the chosen binder, results which could be provided in future by cement manufacturers.

Moreover, as the phenomenological law leads to only three calibration parameters (A_i , B_i and n_i in Eqs (4) and (6)) which differently influence the response of the model, the least squares fitting method allows a precise calibration, whatever the initial values that may be chosen for these three parameters.

5. Model validation

5.1. Temperature evaluation on massive structure in situ

The first validation of the multiphasic model proposed was the temperature prediction of a 27 m³ concrete block in situ, equipped with sensors at its core. The test was performed using a CEM I based concrete with the formulation shown in Table 1.

Cement (CEMI 42,5N)	210 kg/m ³
Fly ash	140 kg/m ³
Sand 0/4mm	763 kg/m ³
Gravel 4/16mm	567 kg/m ³
Gravel 16/32mm	574 kg/m ³
Plasticizer	4 kg/m ³
Effective water	131 kg/m ³

Table 1: Concrete formulation

As this formulation uses composed binder (clinker + fly ash), it is appropriate for the validation of our multicomponent hydration model. The hydration law parameters of the two anhydrous phases were calibrated on this cement type using the method presented in paragraph 4. The fitting parameters are given in Table 2.

		Clinker	Fly Ash
Calibrated values	A _i	1.10E5	1.32E12
	B _i	1.565	7.139
	n _i	0.531	0.172
	ρ _i (kg/m ³)	3224	2200
	R _i (m ³ /m ³)	1.83	1.94
	E _a /R (K ⁻¹)	3200	6800 [8]

Table 2: Hydration kinetics model parameters (Eqs 4 to 10)

As seen in paragraph 3, the hydration law is coupled with a heat balance equation and a water mass balance equation. The thermal and hydric characteristics of the concrete block are thus needed for a coupled simulation. The characteristics used for our formulation of concrete are shown in Tables 3 and 4.

λ	6480	J/(h.m.K)
ρ _c	2190	kJ/(m ³ .K)
Q ^T _{th} clinker	437	J/g
Q ^T _{th} fly ash	570	J/g

Table 3: Thermal characteristics of concrete

Although the formwork and a humid cure prevent hydric transfer between structures and the environment, water movements can occur in concrete blocks. Water consumption by hydration may be different if there are hydration gradients in the structure caused, for instance, by temperature gradients. These movements are managed by Eq. 2 in which D_w is a hydric diffusion coefficient. This coefficient governing water transport is strongly dependent on the moisture content of the pore system. Xi [9] reported this nonlinearity and proposed expressing the diffusion coefficient D_w as a function of relative humidity (y).

$$D_w(y) = D_{w0} \cdot \left(1 + a \cdot \left(1 - 2^{-10^b(y-1)}\right)\right) \quad (13)$$

Where D_{w0} , a and b are model parameters presented in Table 4.

Q_{th}^W clinker	$0.32 \times m_{clinker}$	m^3/m^3
Q_{th}^W fly ash	$0.75 \times m_{fa}$	m^3/m^3
D_{w0}	1E-11	m^2/s
a	6	\emptyset
b	2	\emptyset

Table 4: Hydric characteristics of concrete

The calculations on the structure were performed by implementing the model in the finite element code CASTEM2000 [10]. Figure 1 presents a comparison between model results (curve) and measurements (squares) for the concrete block core temperature variation. It shows that the temperature variation is quite well reproduced by our model.

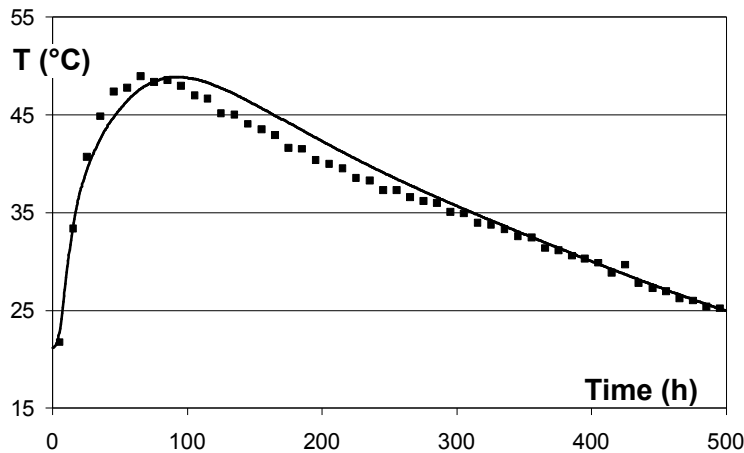


Figure 1: Temperature variations of concrete block core : comparison between experiment (squares) and model (curve)

5.2. Water effects

The relevancy of the proposed multiphasic model was also tested with regard to the prediction of the maximum hydration degree reached by CEM I type cement when it was mixed using different water-to-cement ratios. A comparison was made between the experimental results obtained by Waller [11] and the simulation ones.

Numerical simulations were performed so as to reproduce the experimental conditions used by Waller (adiabatic and autogenous conservation) and for 13 different W/C ratios. The maximum hydration degrees reached are plotted as squares in Figure 2. The curve also present on this figure represents the empirical law fitted by Waller on his numerous experimental results.

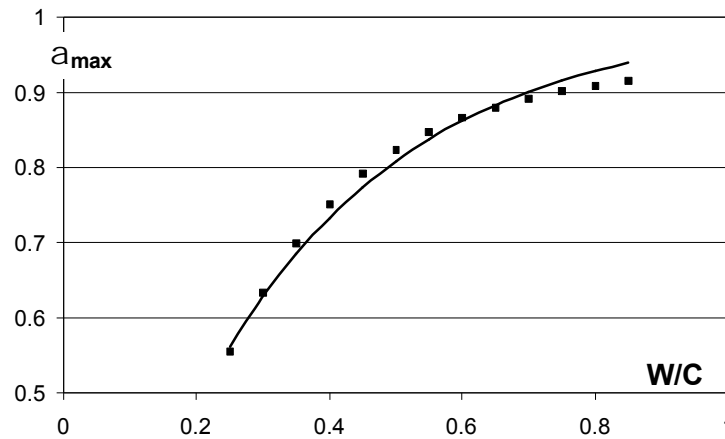


Figure 2: Variation of maximum hydration degree versus W/C ratio: model results (squares) and empirical law [11] (curve)

Figure 2 shows that the hydration law, which was only calibrated on 3 days of quasi adiabatic testing performed using the advocated W/C ratio of 0.5, leads to a maximum hydration degree that matches the empirical law fitted by Waller.

It is interesting to note that the hydration law reproduces this hydration limitation well without explicitly using a factor α_{max} to represent the maximum value of hydration degree, which would have to be given as input data (no possibility of modifying it after casting, by rehydration for instance) [1, 11].

For the model proposed, the water accessibility function ($\Pi(r_m)$) implicitly allows the model to adapt the hydration development to different W/C ratios so as to reach a higher or lower final hydration degree.

It thus also allows the hydration degree to be limited by a parameter other than water, such as decreasing porosity. Moreover, it allows localized hydration development to be changed (even stopped) by desiccation or modified by rehydration.

6. Complementary analysis

6.1. Water effect on hydration kinetics

Figure 3 plots the variations in clinker hydration degree obtained by simulations made with three different water-to-cement ratios (0.4, 0.5, 0.7) in the same curing conditions (autogenous and adiabatic conservation).

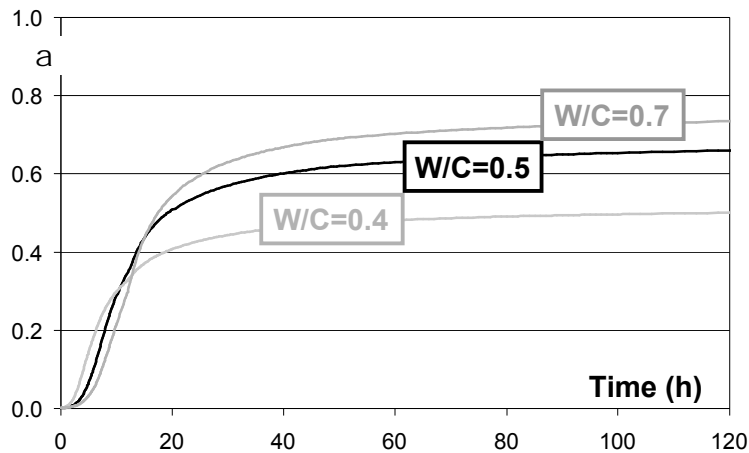


Figure 3: Clinker hydration development for 3 different W/C ratios

In this figure we first note that, after approximately 15 hours, higher W/C ratios give higher hydration degrees, which is conventionally accepted [6]. On the contrary, before 15 hours, a slight increase in hydration kinetics is observed for decreasing W/C ratios. This phenomenon was noticed by Mounanga [12] for low W/C ratios. It can be explained, as seen previously, by supersaturation of the interstitial solution.

Even though this slight modification of initial kinetics does not really affect the temperature field in a massive structure, it is interesting to note that our model reproduces this effect during the early stages of hydration.

6.2. Mineral addition effects

Figure 4 presents the hydration kinetic laws for clinker, expressed according to its hydration degree. The two curves were obtained by simulating two adiabatic tests: the first on a pure CEM I binder and the other on a fly ash composed binder (60% clinker and 40% fly ash).

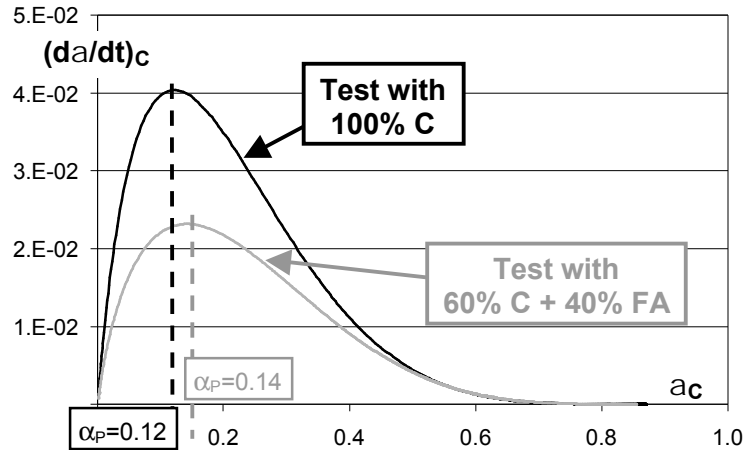


Figure 4: Variation of clinker hydration kinetic law with hydration degree

Figure 4 shows that clinker hydration kinetics is reduced by the partial replacement of cement by fly ash. It also reveals a delaying effect of fly ash on clinker hydration, the kinetic peak being observed for $\alpha=0.14$ in the case of composed binder instead of 0.12 for pure clinker.

This delaying effect has been illustrated experimentally by Schindler [13] and is explained by a consumption of water by the fly ash reaction with portlandite. It highlights the fact that the multiphasic model reproduces the interaction between the reactions of clinker and the additions.

Figure 5 shows the variations of temperature obtained by numerical simulations performed on the concrete test block (27 m^3 cube) used for model validation. Two simulations were performed in order to evaluate the influence of cement replacement rate on temperature development in a massive structure.

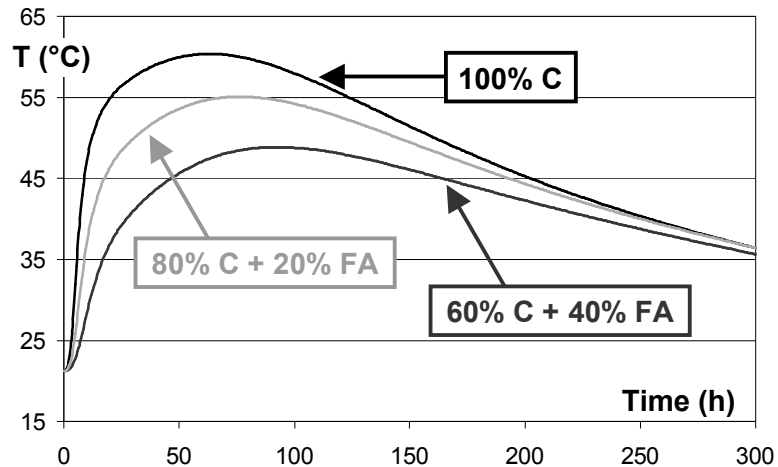


Figure 5: Effect of binder composition on concrete block core temperature

As expected, partial replacement of cement by fly ash reduces the maximum temperature. But the simulation also confirms slower heat development kinetics due to this substitution, as highlighted in Figure 4.

7. Conclusions

This paper is a contribution to the modeling of cementitious material hydration development. The originality of the proposed model is its aptitude to model the hydration of multicomponent binders in realistic conservation conditions (in situ). Indeed, the multiphasic approach allows strong coupling between the hydration development of several species and the temperature and water content of the concrete structure. It was validated, for a binder composed of clinker and fly ash, by temperature measurements on a structure in situ. It was also shown that the model reproduced the effects of initial water content on hydration well. In particular, the maximum hydration degree that can be reached by clinker is estimated with confidence.

8. Acknowledgments

The authors acknowledge the financial support of the French Group *VINCI Construction Grands Projets* (associated with ANRT for CIFRE doctoral scholarship) and particularly thank Laurent Boutillon and Lionel Linger from the Scientific Department for their collaboration and expertise. We are also grateful to *CEA/DEN/DM2S/SEMT* for providing the finite element code CASTEM2000.

- [1] G. De Schutter, Hydration and temperature development of concrete made with blast-furnace slag cement, *Cem Concr Res* 29 (1999) 143-149
- [2] T. Kishi, K. Maekawa, Thermal and mechanical modelling of young concrete based on hydration process of multi-component cement materials, *Thermal cracking in concrete at early age*, Rilem Proceeding 25 (1994) 11-19
- [3] T.C. Powers, T.L. Brownyard, Studies of the physical properties of hardened Portland cement paste, Part 9, *ACI Journal* 18 (8) (1947)
- [4] T. C. Hansen, Physical Structure of Hardened Cement Paste, A Classical Approach, *Mater Struct* 19 (114) (1986) 423-436
- [5] H.F.W. Taylor, *Cement chemistry*, Academic Press, New York, 1990
- [6] D.P. Bentz, Influence of water-to-cement ratio on hydration kinetics: Simple models based on spatial considerations, *Cem Concr Res* 36 (2006) 238-244
- [7] S. Arrhenius, *Quantitative laws in biological chemistry*, G. Bell and Sons, London, 1915
- [8] M.J. Renedo, J. Fernandez, Kinetic modelling of the hydrothermal reaction of fly ash, Ca(OH)_2 and CaSO_4 in the preparation of desulfurant sorbents, *Fuel* 83 (2004) 525-532
- [9] Y. Xi, Z.P. Bazant, L. Molina, H.M. Jennings, Moisture diffusion in cementitious materials: moisture capacity and diffusivity, *Advanced Cement Based Materials* 1 (1994) 258-266
- [10] Commissariat à l'Energie Atomique CEA – DEN/DM2S/SEMT, CASTEM2000, web page: <http://www-cast3m.cea.fr/cast3m/index.jsp>.
- [11] V. Waller, Relations entre composition des bétons, exothermie en cours de prise et résistance en compression, PhD thesis (1999), ENPC Paris, 297p
- [12] P. Mounanga, Comportement des matrices cimentaires au jeune âge : relation entre évolution chimique et déformations chimique et endogène. XXIEMES Rencontres Universitaires de Génie Civil. (2003)
- [13] A.K. Schindler, K.J. Folliard, Influence of supplementary cementing materials on the heat of hydration of concrete, *Advances in Cement and Concrete IX Conference*, Colorado, August 2003, 10p